OPEN ACCESS • OPEN ACCESS

Relationship between charge density wave, filamentary superconductivity and bulk superconductivity in $ZrTe_3$

To cite this article: A. Nomura *et al* 2021 *EPL* **133** 37003

A Letters Journal Exploring the Frontiers of Physics

February 2021

EPL, **133** (2021) 37003
doi: 10.1209/0295-5075/133/37003

www.epljournal.org

Relationship between charge density wave, filamentary superconductivity and bulk superconductivity in $ZrTe_3$

A. Nomura, S. Kobayashi, S. Ohta and H. Sakata

Department of Physics, Tokyo University of Science - Shinjuku, Tokyo 162-8601, Japan

received 3 July 2020; accepted in final form 5 January 2021
published online 26 March 2021

PACS 74.70.-b – Superconducting materials other than cuprates
PACS 71.45.Lr – Charge-density-wave systems
PACS 74.25.Dw – Superconductivity phase diagrams

Abstract – We investigated the relationship between a charge density wave (CDW) with a transition temperature (T_{CDW}) of ∼60 K, filamentary superconductivities (SCs) along the a-axis and the b-axis with transition temperatures (T_C's) of ∼3.5 K, and a bulk SC with a T_C below 2.5 K in $ZrTe_3$, by measuring electrical resistance and magnetization for several crystals synthesized at different growth temperatures. As the growth temperature increased, the T_{CDW} decreased, the T_C of the bulk SC increased, and the T_C's of the filamentary SCs did not show a clear change. The anisotropy of the upper critical field (H_{C2}) was different between the filamentary SCs and the bulk SC. These differences in the growth temperature dependence of T_C and the anisotropy of H_{C2} indicate that the filamentary SCs are unrelated to the bulk SC. Moreover, the growth temperature dependence of the transition temperatures indicates that the CDW has a competitive relationship with the bulk SC, but a non-competitive coexistence with the filamentary SCs. Based on the anisotropies of H_{C2}, we also infer that the filamentary SCs and the bulk SC occur on quasi-one-dimensional Fermi surfaces and a three-dimensional Fermi surface, respectively, and that the relationship between the three states in $ZrTe_3$ cannot be explained solely in terms of conventional competition for a Fermi surface.

Introduction. – Superconductivity (SC) is an ordered state of electrons in metals at low temperatures with formation of an energy gap on a Fermi surface (FS). SC generally exhibits effects such as zero electric resistance, complete diamagnetism, and a jump in specific heat. However, an atypical form of SC also exists, having zero electric resistance but no bulk superconducting properties such as complete diamagnetism and/or a jump in specific heat, and is referred to as filamentary SC. For some materials, filamentary SC is considered to be local SC caused by an inhomogeneous composition of a crystal [1]. On the other hand, in materials exhibiting a filamentary SC transition at a higher temperature and a bulk SC transition at a lower temperature, it has been proposed that filamentary SC is a precursor to bulk SC, indicating an unconventional superconducting mechanism [2–4]. However, the validity of this suggestion remains unclear because direct evidence has not been obtained.

Charge density wave (CDW) is another ordered state of electrons with an energy gap on an FS. The relationship between SC and CDW has been investigated in many materials by changing their properties by impurity doping or pressure application. Most of these results showed that either SC or a CDW is enhanced while the other is suppressed, which has been ascribed to competition for an FS by SC and CDW [5,6]. On the other hand, a recent study proposed that CDW is not necessarily in competition with SC [7]. Moreover, another study suggested that the incommensuration of CDW may affect the relationship between SC and CDW [8]. Therefore, there may be a mechanism that defines the relationship between CDW and SC besides competition for an FS, and the relationship between the two states is still a major research topic in condensed matter physics.

$ZrTe_3$ provides a stage to address the above open questions. $ZrTe_3$ is a low-dimensional material with a

chain structure along the b-axis, and has flat quasi-one-dimensional Fermi surfaces (q1D FSs) perpendicular to the a^*-direction, and a cylindrical three-dimensional Fermi surface (3D FS) along the c'^*-direction [9–11]. $ZrTe_3$ exhibits a CDW transition at ∼63 K, with a corresponding increase in resistance along the a-axis and the c'-axis but no increase along the b-axis [12]. The CDW vector is (1/14, 0, 1/3) according to the result of electron diffraction [13]. From this anisotropic increase in resistance and the CDW vector, it is evident that the CDW forms on the q1D FSs. Furthermore, $ZrTe_3$ exhibits a filamentary SC transition and a bulk SC transition below 4 K. It was reported that the resistance along the a-axis fell to zero at 2–4 K [2,3,14]. On the other hand, at the same temperature, the resistance along the b-axis did not decrease, and no detectable diamagnetic signal was observed by magnetic susceptibility measurements. From these results, a model for the filamentary SC along the a-axis was proposed. In addition, a superconducting specific-heat jump was observed at ∼1.3 K, indicating a bulk SC transition [2].

The relationship between the CDW, the filamentary SC and the bulk SC in $ZrTe_3$ has been investigated in previous studies [2,3,15–17]. For example, the filamentary SC and the bulk SC were investigated by measurement of resistance and specific heat [2,3]. Based on the results, it was proposed that the filamentary SC is a precursor to the bulk SC. Moreover, it was reported that substitution of a small amount of Se atoms for Te atoms suppresses the CDW and enhances a bulk SC, showing the competition between the CDW and the bulk SC [15]. However, the whole picture of the relationship between the three states remains unclear due to the following problems: i) The filamentary SC and the bulk SC were not distinguished in some previous studies. ii) No experimental results have been obtained to determine the relationship between the filamentary SC and the bulk SC. iii) The knowledge obtained in previous studies relates to the relationship between two of the three states, and is fragmentary. iv) It has not been determined where the SCs occur on the FSs. This information is important for discussing the relationship between the CDW and the SCs, because they are associated with opening of an energy gap on the FSs.

To solve the above problems in $ZrTe_3$, we observed the CDW transition and the filamentary SC transition by electrical resistance measurements and the bulk SC transition by magnetization measurements separately in the present study. Specifically, we measured the transition temperatures of the three states for several $ZrTe_3$ crystals synthesized at different growth temperatures, and investigated the relationship between the three states by comparing the growth temperature dependence of the transition temperatures. It was reported that the growth temperature can be used as a tuning parameter to vary the CDW and the bulk SC in $ZrTe_3$ [17]. Furthermore, the anisotropies of upper critical field (H_{C2}) for the filamentary SC and the bulk SC were measured in the present study to investigate the relationship between the SCs, and where the SCs occur on the FSs because H_{C2} contains information about the FS where SC forms.

Experimental. – We prepared four kinds of $ZrTe_3$ single crystals synthesized at 740, 780, 820, and 860 °C by vapor phase transport. First, we sealed the materials of Zr (0.354 g, 99.9%), Te (1.483 g, 99.999%) and I (4 mg/cc, 99.8%) in four evacuated quartz tubes with inner diameters of 1.5 cm and lengths of 18 cm. Each tube was then heated so that the temperature of materials at one end of the tube was 740, 780, 820, or 860 °C, and the temperature at the other end was 40 °C lower. The reason for making the temperature gradient smaller than that of previous reports (∼100 °C) is to obtain crystals formed at almost the same temperature from one tube. After maintained at the temperature for seven days, the tubes were quenched in water. In this way, we obtained single crystals with typical dimension of 0.5 mm × 1 mm × 0.05 mm at the hotter end. It was confirmed by single-crystal X-ray diffraction that the crystals were $ZrTe_3$.

The temperature dependence of the resistance along the a-axis and b-axis from 2 to 280 K was measured using a dc four-probe technique. Two ribbon-shaped fragments whose longest sides were along the a-axis and the b-axis were cut from one crystal. We measured the resistance along the longest side of each fragment while heating from 2 to 280 K. The temperature was measured using a Cernox resistance sensor. Moreover, for $ZrTe_3$(860 °C), we measured the resistance under static magnetic fields (0–6 T) parallel to the a-axis, b-axis and c'-axis after zero-field cooling.

The magnetic properties were measured using a MPMS SQUID magnetometer (Quantum Design). For $ZrTe_3$(740 °C) and $ZrTe_3$(860 °C), we used the part of the crystal remaining after removing samples for the resistance measurements. The temperature dependence of the magnetic susceptibility (χ) was measured from 1.8 to 8 K, applying a static magnetic field of 2 G parallel to the a-axis. In addition, the magnetic field dependence of the magnetization was measured at 2 K. The magnetic field was applied parallel to the a-axis, b-axis and c'-axis.

Results. – Figure 1 shows the results of resistance measurements along the a-axis and b-axis for $ZrTe_3$(740 °C), $ZrTe_3$(780 °C), $ZrTe_3$(820 °C), and $ZrTe_3$(860 °C). As shown in fig. 1(a), (c), (e), (g), all the samples showed an anisotropic temperature dependence of the resistance above 5 K, as seen in previous studies [3,12,17]. The resistance along the a-axis showed an increase at about 60 K due to the CDW transition. The temperature derivative of the resistance (dR/dT) along the a-axis showed a dip corresponding to the resistance increase as shown in the inset. We define the CDW transition temperature (T_{CDW}) as the temperature at which the dR/dT drops most, because the opening of a CDW gap at T_{CDW} causes a sharp drop in dR/dT in CDW conductors [18]. As shown in fig. 1(i), the T_{CDW} decreased with increasing growth

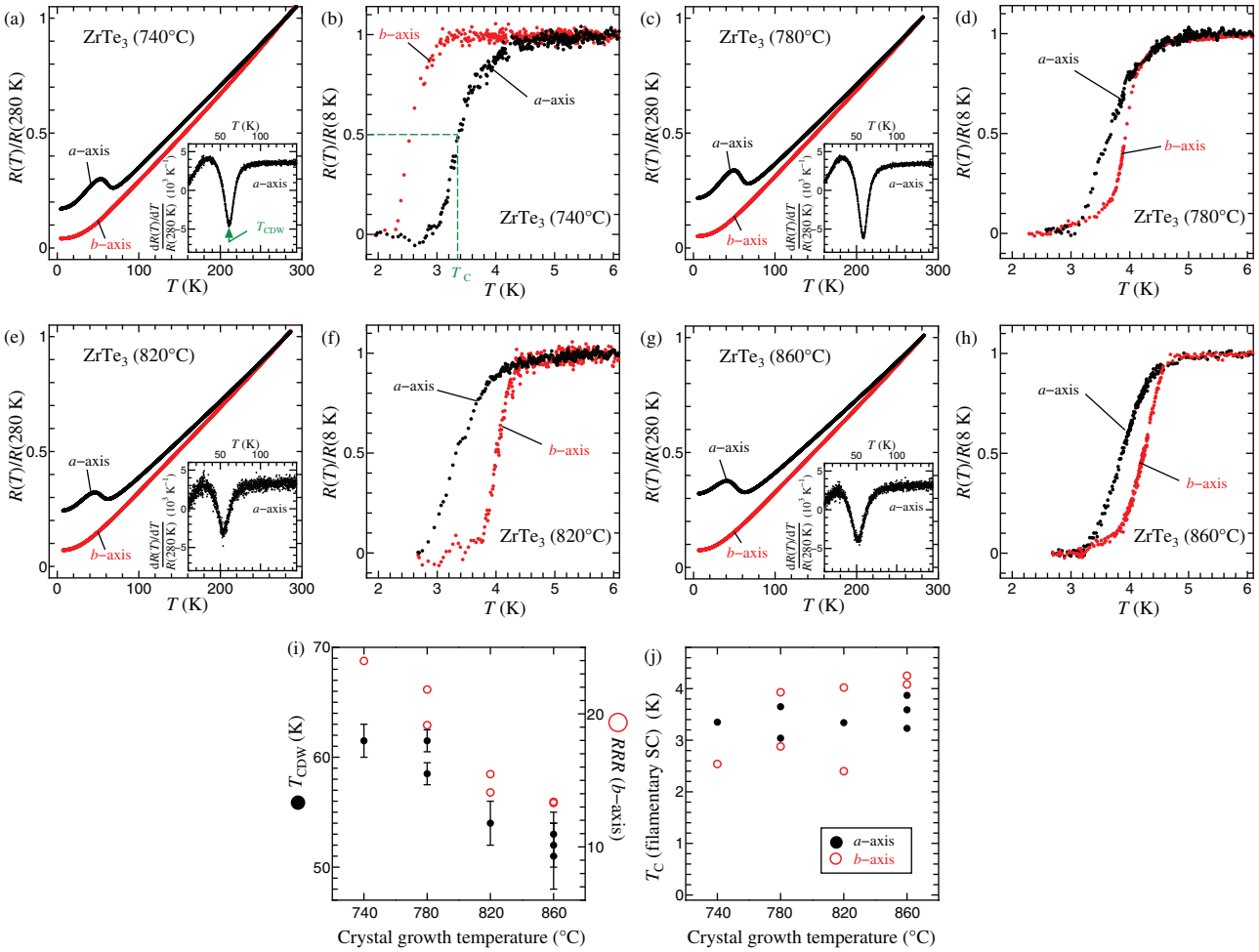

Fig. 1: Results of resistance measurements along the a-axis and b-axis for $ZrTe_3$(740 °C), $ZrTe_3$(780 °C), $ZrTe_3$(820 °C), and $ZrTe_3$(860 °C). (a), (c), (e), (g): typical temperature dependence of the resistance from 8 to 280 K normalized by the resistance at 280 K. The inset shows the temperature derivative of the resistance (dR/dT) normalized by the resistance at 280 K along the a-axis. T_{CDW} is defined as the temperature at which the dR/dT drops most. (b), (d), (f), (h): typical temperature dependence of the resistance below 6 K normalized by the resistance at 8 K. The measurement below 8 K was performed with a smaller current than that above 8 K. T_C is defined as the temperature at which $R(T)/R(8\,\mathrm{K}) = 0.5$. The current density was several hundred milliamperes and several amperes per square centimeter for the measurement along the a-axis and b-axis, respectively. When the current density was further reduced, the change in T_C was at most 0.1 K. (i) T_{CDW} and $RRR(= R(280\,\mathrm{K})/R(8\,\mathrm{K}))$ along the b-axis as a function of crystal growth temperature. (j) T_C's for the filamentary SCs along the a-axis and the b-axis as a function of crystal growth temperature.

temperature. The resistance along the b-axis showed a metallic temperature dependence over the entire temperature range above 5 K (fig. 1(a), (c), (e), (g)). The residual resistance ratio ($RRR = R(280\,\mathrm{K})/R(8\,\mathrm{K})$) decreased with increasing growth temperature (fig. 1(i)), which is consistent with a previous report that high growth temperature induces lattice disorder [17]. As shown in fig. 1(b), (d), (f), (h), all the samples exhibited a sharp drop in resistance along the a-axis and b-axis below 5 K due to the SC transition. The SC transition temperatures (T_C's) along both axes did not show a clear change with increasing growth temperature as shown in fig. 1(j).

Figure 2(a)–(f) shows the temperature dependence of the resistance below 6 K under various magnetic fields for $ZrTe_3$(860 °C). The T_C's along the a-axis and b-axis decreased as the magnetic field in each direction increased. Figure 2(g), (h) shows the temperature dependence of the H_{C2}'s. We define H_{C2} for $R(T)/R(8\,\mathrm{K}) = 0.5$. It is considered that the demagnetization has almost no effect on the H_{C2}'s because the demagnetizing field is much smaller than the applied magnetic field when SC breaks. In both the $I \parallel a$ and $I \parallel b$ cases, the H_{C2}'s increased in the order c'-axis, b-axis and a-axis. The ratios for H_{C2}'s at 2 K are expressed as

$$I \parallel a \quad H_{C2\,a} : H_{C2\,b} : H_{C2\,c'} = 2.96\,\mathrm{T} : 0.66\,\mathrm{T} : 0.40\,\mathrm{T} = 1 : 0.22 : 0.14, \tag{1}$$

$$I \parallel b \quad H_{C2\,a} : H_{C2\,b} : H_{C2\,c'} = 5.13\,\mathrm{T} : 2.71\,\mathrm{T} : 1.48\,\mathrm{T} = 1 : 0.53 : 0.29. \tag{2}$$

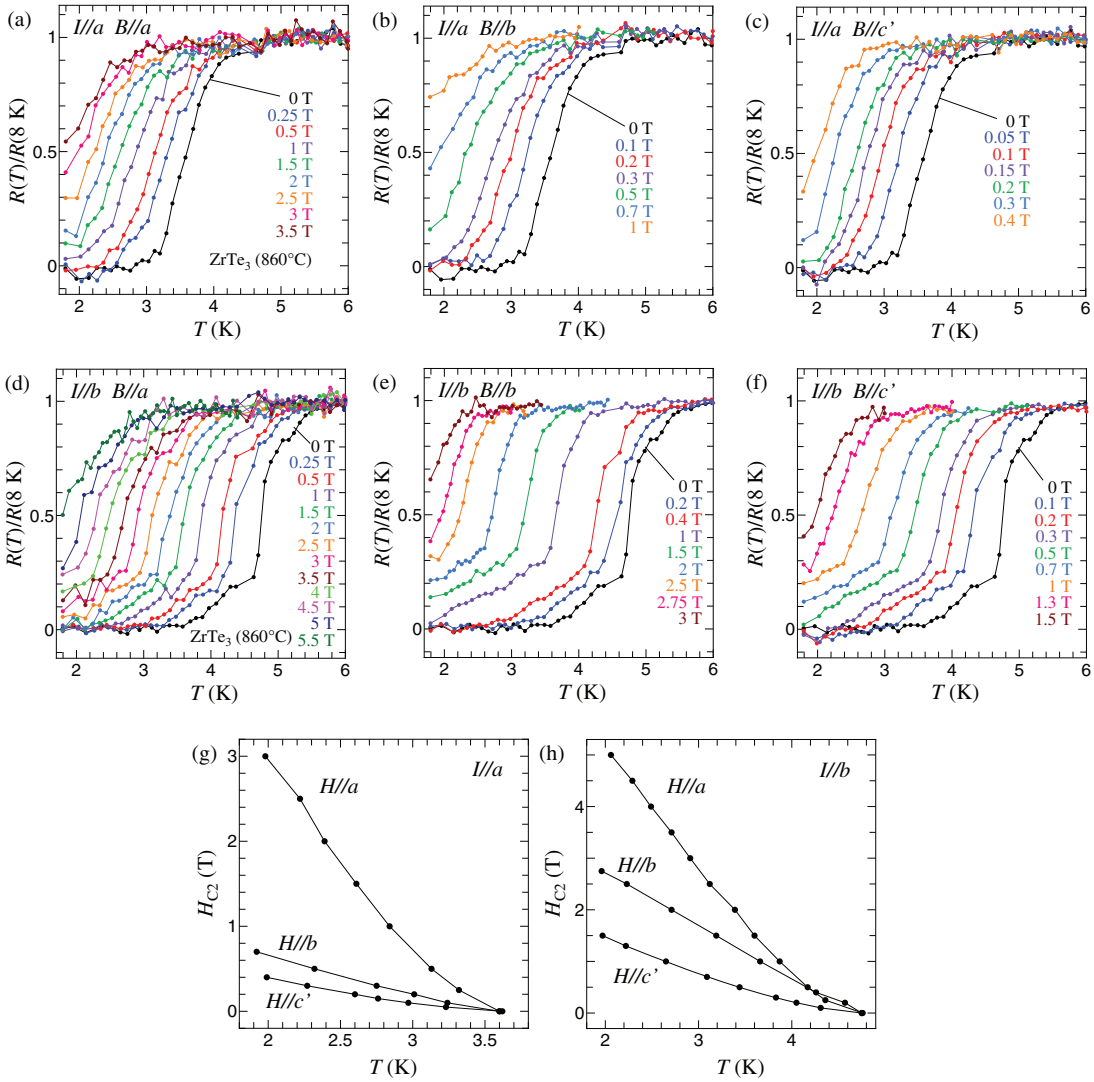

Fig. 2: (a) Temperature dependence of the resistance of $ZrTe_3$(860 °C) under various magnetic fields. The current (or resistance) is along the a-axis, and the field is parallel to the a-axis ($I \parallel a$, $H \parallel a$). (b) $I \parallel a$, $H \parallel b$. (c) $I \parallel a$, $H \parallel c'$. (d) $I \parallel b$, $H \parallel a$. (e) $I \parallel b$, $H \parallel b$. (f) $I \parallel b$, $H \parallel c'$. (g), (h): temperature dependence of the H_{C2}'s parallel to the a-axis, b-axis, and c'-axis for $ZrTe_3$(860 °C), obtained from resistance measurements for $I \parallel a$ and $I \parallel b$. We define H_{C2} for $R(T)/R(8\,\mathrm{K}) = 0.5$.

Thus, the ratio for H_{C2}'s parallel to the a-axis, b-axis and c'-axis was different in the $I \parallel a$ and $I \parallel b$ cases, although the order of H_{C2}'s was the same.

Figure 3(a) shows the temperature dependence of the χ. $ZrTe_3$(860 °C) and $ZrTe_3$(820 °C) exhibited a remarkable decrease in χ due to a bulk SC transition below 2.5 K. $ZrTe_3$(780 °C) exhibited a slight decrease below 2 K and $ZrTe_3$(740 °C) exhibited no decrease. Figure 3(b) shows the magnetization as a function of magnetic field at 2 K for $ZrTe_3$(860 °C). Magnetic hysteresis was observed for each magnetic field direction as shown in the inset, indicating type-II superconductivity. As shown in the whole graph, when the magnetic field increased, the absolute value of the magnetization along the c'-axis decreased most rapidly and that along the a-axis decreased as rapidly as that along the b-axis. For example, when the magnetization is $-0.01\,\mathrm{emu/cm^3}$, the magnetic field parallel to the a-axis, the b-axis and the c'-axis was 585, 555 and 296 Oe, respectively. Thus, the anisotropy of H_{C2} at 2 K is expressed as

$$H_{C2\,a} \approx H_{C2\,b} > H_{C2\,c'}, \tag{3}$$

although it is difficult to determine the values of H_{C2} from the magnetic hysteresis.

Discussion. – In the temperature dependence of the resistance, all the samples exhibited an SC transition at ∼3.5 K (see fig. 1(b), (d), (f), (h), (j)). On the other hand, in the temperature dependence of the χ, $ZrTe_3$(740 °C) and $ZrTe_3$(780 °C) did not exhibit a clear diamagnetic signal due to an SC transition, while $ZrTe_3$(820 °C) and $ZrTe_3$(860 °C) did below 2.5 K (fig. 3(a)). From these results, the SC transition in the R-T curve indicates a filamentary SC transition and that in the χ-T curve indicates

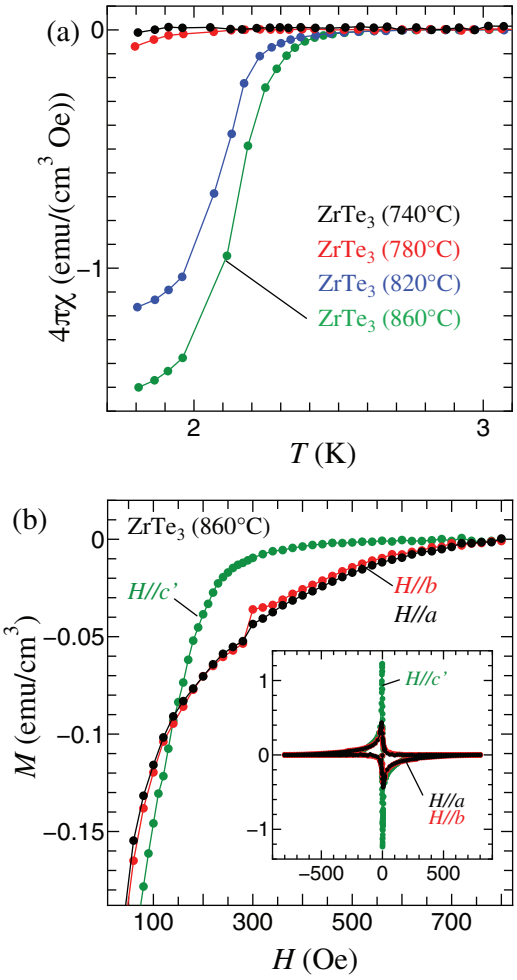

Fig. 3: (a) Temperature dependence of the magnetic susceptibility (χ) during heating after zero-field cooling for $ZrTe_3$(740 °C), $ZrTe_3$(780 °C), $ZrTe_3$(820 °C), and $ZrTe_3$(860 °C). The applied magnetic field is 2 G and parallel to the a-axis. We obtained the χ without a demagnetization factor correction. (b) Magnetization as a function of magnetic field at 2 K for $ZrTe_3$(860 °C) when the magnetic field increases. The inset shows the whole magnetic hysteresis loop. We subtracted the background magnetization.

a bulk SC transition. Thus, we observed the filamentary SC and the bulk SC separately.

In previous studies, the filamentary SC transition has been observed in the R-T curve only along the a-axis, and the SC is considered to be composed of superconducting filaments along the a-axis [2,3,14]. On the other hand, we found a filamentary SC transition in the R-T curves not only along the a-axis but also along the b-axis (fig. 1(b), (d), (f), (h)). Furthermore, the ratio for H_{C2}'s parallel to the a, b and c'-axes varied depending on whether $I \parallel a$ or $I \parallel b$ (eqs. (1), (2)). These results suggest that another filamentary SC extending along the b-axis develops in addition to that along the a-axis in our samples.

Possible explanations for the identity of the filamentary SCs along the a-axis and the b-axis include a local SC caused by the inhomogeneity of T_C for the bulk SC, a fluctuation or precursor of the bulk SC, and an SC with a filament structure unrelated to the bulk SC. In our results, for the filamentary SCs, the H_{C2}'s increased in the order c'-axis, b-axis and a-axis (fig. 2(g), (h), eqs. (1), (2)). On the other hand, for the bulk SC, the H_{C2} parallel to the a-axis and that parallel to the b-axis were almost the same and that parallel to the c'-axis was the smallest (eq. (3)). The samples used for these H_{C2} measurements were prepared from the same crystal. Moreover, as the growth temperature increased, the T_C's for the filamentary SCs did not show a clear change while the T_C for the bulk SC decreased (fig. 1(j), fig. 3(a)). Based on these differences in the anisotropy of H_{C2} and the growth temperature dependence of T_C, the filamentary SCs can be identified as SCs with filament structures unrelated to the bulk SC.

We discuss the relationship between the CDW and the SCs. The CDW was suppressed while the bulk SC was enhanced as the growth temperature increased (fig. 1(i), fig. 3(a)). This result indicates that the CDW and the bulk SC compete. On the other hand, the T_C's for the filamentary SCs were independent of growth temperature (fig. 1(j)). This indicates that the CDW coexists non-competitively with the filamentary SCs.

We discuss where the filamentary and bulk SCs occur on the FS from the anisotropies of H_{C2}. We found that the anisotropies of H_{C2} for the SCs are as expressed in eqs. (1)–(3). Based on the anisotropic Ginzburg-Landau theory, the anisotropy of H_{C2} is expressed as

$$H_{C2\,a} : H_{C2\,b} : H_{C2\,c'} = \frac{\phi_0}{2\pi\xi_b\xi_{c'}} : \frac{\phi_0}{2\pi\xi_{c'}\xi_a} : \frac{\phi_0}{2\pi\xi_a\xi_b} = \xi_a : \xi_b : \xi_{c'}, \tag{4}$$

where ϕ_0 is flux quantum, and ξ_a, ξ_b and $\xi_{c'}$ are the coherence lengths in the a-axis, b-axis and c'-axis, respectively. When the SC gap is isotropic and there is no decrease in ξ due to a short mean-free path and the small size of superconductor, ξ is proportional to the Fermi velocity (v_F) according to the Pippard's model, and therefore the anisotropy of H_{C2} is expressed as

$$H_{C2\,a} : H_{C2\,b} : H_{C2\,c'} \approx v_{Fa} : v_{Fb} : v_{Fc'}. \tag{5}$$

Applying eq. (5) to eqs. (1)–(3), the anisotropies of v_F for the filamentary SCs and the bulk SC are expressed as

filamentary SC (a-axis),
$$v_{Fa} : v_{Fb} : v_{Fc'} \approx 1 : 0.22 : 0.14, \tag{6}$$
filamentary SC (b-axis),
$$v_{Fa} : v_{Fb} : v_{Fc'} \approx 1 : 0.53 : 0.29, \tag{7}$$
bulk SC,
$$v_{Fa} \approx v_{Fb} > v_{Fc'}, \tag{8}$$

assuming isotropic SC gaps and no decrease in ξ's. $ZrTe_3$ has flat q1D FSs perpendicular to a^* and a cylindrical

3D FS along c'^* [9–11]. It is expected that the $v_{\mathrm{F}a}$ is much larger than the $v_{\mathrm{F}b}$ and the $v_{\mathrm{F}c'}$ on the q1D FSs and the $v_{\mathrm{F}c'}$ is much smaller than $v_{\mathrm{F}a}$ and $v_{\mathrm{F}b}$ on the 3D FS. Therefore, eqs. (6)–(8) imply that the filamentary SCs and the bulk SC occur on the q1D FSs and the 3D FS, respectively. Because of the difference in the ratios for v_{F}'s, the places where the filamentary SCs along the a-axis and the b-axis develop may be different on the remainder of the q1D FSs after the CDW transition.

From the growth temperature dependence of the transition temperatures and the discussion on FSs, we infer that the CDW and the bulk SC compete in $ZrTe_3$ although the CDW and the bulk SC occur on the q1D FSs and the 3D FS, respectively. Moreover, it is implied that the filamentary SCs along the a-axis and the b-axis which occur on the q1D FSs coexist non-competitively with the CDW and the bulk SC. This relationship cannot be explained solely in terms of competition for an FS and there may be another mechanism that defines the relationship between CDW and SC.

Conclusion. – We investigated the relationship between the CDW, the filamentary SCs and the bulk SC in $ZrTe_3$ by measuring resistance and magnetization for crystals synthesized at 740, 780, 820, and 860 °C. The resistance along the a-axis showed an increase at 51–62 K due to the CDW transition, and the T_{CDW} decreased with increasing growth temperature. The resistance along both the a-axis and b-axis exhibited a sharp drop at ~ 3.5 K due to the filamentary SC transitions, and the T_{C}'s were independent of the growth temperature. The H_{C2} values obtained by resistance measurements under a magnetic field increased in the order c'-axis, b-axis and a-axis for both $I \parallel a$ and $I \parallel b$, but the ratio for H_{C2}'s parallel to the a, b and c'-axes varied for $I \parallel a$ or $I \parallel b$. The zero resistance along the b-axis and the difference in the ratios for H_{C2}'s suggest that another filamentary SC extending along the b-axis develops in addition to that along the a-axis in our samples. The samples synthesized at 820 °C and 860 °C exhibited a remarkable decrease in χ due to the bulk SC transition below 2.5 K, but the samples synthesized at 740 °C and 780 °C did not. The magnetic hysteresis showed that the H_{C2} for the bulk SC parallel to the a-axis and that parallel to the b-axis were almost the same, and that parallel to the c'-axis was the smallest. Based on the differences in the anisotropy of H_{C2} and the growth temperature dependence of T_{C} between the filamentary SCs and the bulk SC, the filamentary SCs can be identified as SCs with filament structures unrelated to the bulk SC. The growth temperature dependences of transition temperature indicate that the CDW has a competitive relationship with the bulk SC, but coexists non-competitively with the filamentary SCs. From the anisotropies of H_{C2}, we infer that the filamentary SCs and the bulk SC occur on the q1D FSs and the 3D FS, respectively.

REFERENCES

[1] Gofryk K., Pan M., Cantoni C., Saparov B., Mitchell J. E. and Sefat A. S., *Phys. Rev. Lett.*, **112** (2014) 047005.

[2] Yamaya K., Takayanagi S. and Tanda S., *Phys. Rev. B*, **85** (2012) 184513.

[3] Tsuchiya S., Matsubayashi K., Yamaya K., Takayanagi S., Tanda S. and Uwatoko Y., *New J. Phys.*, **19** (2017) 063004.

[4] Xiao H., Hu T., He S. K., Shen B., Zhang W. J., Xu B., He K. F., Han J., Singh Y. P., Wen H. H., Qiu X. G., Panagopoulos C. and Almasan C. C., *Phys. Rev. B*, **86** (2012) 064521.

[5] Kawabata K., *J. Phys. Soc. Jpn.*, **54** (1985) 762.

[6] Sipos B., Kusmartseva A. F., Akrap A., Berger H., Forró L. and Tutiš E., *Nat. Mater.*, **7** (2008) 960.

[7] Nomura A., Yamaya K., Takayanagi S., Ichimura K. and Tanda S., *EPL*, **124** (2018) 67001.

[8] Kogar A., de la Pena G. A., Lee S., Fang Y., Sun S. X.-L., Lioi D. B., Karapetrov G., Finkelstein K. D., Ruff J. P. C., Abbamonte P. and Rosenkranz S., *Phys. Rev. Lett.*, **118** (2017) 027002.

[9] Lyu S.-P., Yu L., Huang J.-W., Lin C.-T., Gao Q., Liu J., Liu G.-D, Zhao L., Yuan J., Chen C.-T., Xu Z.-Y. and Zhau X.-J., *Chin. Phys. B*, **27** (2018) 087503.

[10] Hoesch M., Cui X., Shimada K., Battaglia C., Fujimori S.-i. and Berger H., *Phys. Rev. B*, **80** (2009) 075423.

[11] Hoesch M., Gannon L., Shimada K., Parrett B. J., Watson M. D., Kim T. K., Zhu X. and Petrovic C., *Phys. Rev. Lett.*, **122** (2019) 017601.

[12] Takahashi S., Sambongi T., Brill J. W. and Roark W., *Solid State Commun.*, **49** (1984) 1031.

[13] Eaglesham D. F., Steeds J. W. and Wilson J. A., *J. Phys. C: Solid State Phys.*, **17** (1984) L697.

[14] Nakajima H., Nomura K. and Sambongi T., *Physica B*, **143** (1986) 240.

[15] Zhu X., Ning W., Li L., Ling L., Zhang R., Zhang J., Wang K., Liu Y., Pi L., Ma Y., Du H., Tian M., Sun Y., Petrovic C. and Zhang Y., *Sci. Rep.*, **6** (2016) 26974.

[16] Yomo R., Yamaya K., Abliz M., Hedo M. and Uwatoko Y., *Phys. Rev. B*, **71** (2005) 132508.

[17] Zhu X., Lv B., Wei F., Xue Y., Lorenz B., Deng L., Sun Y. and Chu C.-W., *Phys. Rev. B*, **87** (2013) 024508.

[18] Nomura A., Yamaya K., Takayanagi S., Ichimura K., Matsuura T. and Tanda S., *EPL*, **119** (2017) 17005.